Therapeutic Discovery

Molecular Cancer Therapeutics

Effective Targeting of Hedgehog Signaling in a Medulloblastoma Model with PF-5274857, a Potent and Selective Smoothened Antagonist That Penetrates the Blood–Brain Barrier

Allison Rohner[1], Mary E. Spilker[2], Justine L. Lam[2], Bernadette Pascual[1], Darian Bartkowski[2], Qing John Li[1], Amy H. Yang[3], Greg Stevens[3], Meirong Xu[1], Peter A. Wells[1], Simon Planken[4], Sajiv Nair[4], and Shaoxian Sun[1]

Abstract

Inhibition of the Smoothened (Smo) represents a promising therapeutic strategy for treating malignant tumors that are dependent on the Hedgehog (Hh) signaling pathway. PF-5274857 is a novel Smo antagonist that specifically binds to Smo with a K_i of 4.6 ± 1.1 nmol/L and completely blocks the transcriptional activity of the downstream gene *Gli1* with an IC_{50} of 2.7 ± 1.4 nmol/L in cells. This Smo antagonist showed robust antitumor activity in a mouse model of medulloblastoma with an *in vivo* IC_{50} of 8.9 ± 2.6 nmol/L. The downregulation of Gli1 is closely linked to the tumor growth inhibition in patched$^{+/-}$ medulloblastoma mice. Mathematical analysis of the relationship between the drug's pharmacokinetics and Gli1 pharmacodynamics in patched$^{+/-}$ medulloblastoma tumor models yielded similar tumor and skin Gli1 IC_{50} values, suggesting that skin can be used as a surrogate tissue for the measurement of tumor Gli1 levels. In addition, PF-5274857 was found to effectively penetrate the blood–brain barrier and inhibit Smo activity in the brain of primary medulloblastoma mice, resulting in improved animal survival rates. The brain permeability of PF-5274857 was also confirmed and quantified in nontumor-bearing preclinical species with an intact blood–brain barrier. PF-5274857 was orally available and metabolically stable *in vivo*. These findings suggest that PF-5274857 is a potentially attractive clinical candidate for the treatment of tumor types including brain tumors and brain metastasis driven by an activated Hh pathway. *Mol Cancer Ther; 11(1); 57–65. ©2011 AACR.*

Introduction

The Hedgehog (Hh) signaling pathway plays a critical role in proliferation and differentiation during embryogenesis and early development to ensure proper embryonic patterning in tissues (1). The signaling is initiated by Hh ligand binding to the receptor Patched 1 (Ptch1), which relieves the suppression of Smoothened (Smo; ref. 2). The activated Smo triggers nuclear translocation of transcription factors Gli and initiates transcription of Hh-responsive genes (3).

Although Hh signaling activity is significantly reduced in normal adulthood, it can be aberrantly activated through sporadic mutations or other mechanisms, thereby contributing to the development of a variety of tumor malignancies (4). For example, basal cell carcinoma has a high frequency of inactivating mutations in PTCH1 or to a lesser extent, activating mutations in SMO (5–8). Approximately 20% of medulloblastoma tumors harbor loss-of-function mutations of PTCH1 (9–11). In addition, there is increasing evidence that links the activated Hh pathway to pancreatic (12–16), hematologic (17, 18), and small cell lung cancers (19, 20) among others. Because of its crucial role in tumorigenesis, the Hh pathway draws great interest as a potential therapeutic target (21, 22). Several small-molecule inhibitors have been identified and are currently being evaluated in clinical trials (23, 24). Most of inhibitors directly target Smo as the major component of the Hh pathway (25).

Here, we report a potent and highly selective Smo antagonist PF-5274857 with pharmaceutical properties suitable for clinical development. In addition, this molecule is likely to penetrate the blood–brain barrier in humans, which may offer clinical benefits in treating patients with brain tumors or brain metastasis of primary tumors driven by the activated Hh pathway. Here, we describe the compound's antitumor efficacy in a medulloblastoma tumor model, a correlation of its pharmacokinetic (PK) and pharmacodynamic (PD) properties, and

Authors' Affiliations: [1]Oncology Research Unit, [2]Pharmacokinetics, Dynamics and Metabolism, [3]Drug Safety Research and Development, and [4]Cancer Chemistry, Pfizer Worldwide Research and Development, La Jolla Laboratories, San Diego, California

Note: Supplementary data for this article are available at Molecular Cancer Therapeutics Online (http://mct.aacrjournals.org/).

Corresponding Author: Shaoxian Sun, Oncology Research Unit, Pfizer Worldwide Research and Development, La Jolla Laboratories, 10724 Science Center Drive, San Diego, CA 92121. Phone: 858-526-4922; Fax: 858-526-4275; E-mail: shaoxian.sun@pfizer.com

doi: 10.1158/1535-7163.MCT-11-0691

characterization of its brain penetration in preclinical models.

Materials and Methods

Compounds

PF-5274857 [1-[4-(5′-chloro-3,5-dimethyl-2,4′-bipyridin-2′-yl)piperazin-1-yl]-3-(methylsulfonyl)propan-1-one] was designed and synthesized at Pfizer Worldwide Research and Development. The chemical structure is shown in Fig. 1A. The compound was dissolved in dimethyl sulfoxide for the *in vitro* assays and formulated in 0.5% methylcellulose for *in vivo* studies. The tritium-labeled Smo antagonist (the des-chloro derivative of compound Z in refer. 26) was prepared at the Pfizer Groton facility.

Cell lines

HEK293FlpIn-TetR cells (Invitrogen) were used to stably express human Smo by Flp recombinase–mediated insertion of the pSecTag-FRT/V5-His vector containing a cDNA encoding amino acids 181 to 787 of human Smo. Gli-Luc mouse embryonic fibroblast (MEF) cells containing a luciferase reporter gene under the control of Gli response element were isolated from Gli-Luc transgenic mice at the Pfizer Groton facility. All cell lines were tested by the University of Missouri Research Animal Diagnostic Laboratory for known species of murine viruses and Mycoplasma contamination. Cell authentication was not done by the authors within the last 6 months.

Biochemical assays

HEK293 cells overexpressing human Smo (amino acids 181–787) were grown in Dulbecco's Modified Eagle's Media (DMEM) supplemented with 10% FBS (Invitrogen), Pen–Strep, and 0.1 mg/mL hygromycin to 90% confluence. After washing with cold Dulbecco's PBS, the cell pellet was resuspended in membrane preparation buffer (50 mmol/L Tris-HCl, pH 7.5, 250 mmol/L sucrose with Roche complete protease cocktail) and homogenized. The homogenate was centrifuged and the cell pellet was resuspended in assay buffer (50 mmol/L Tris-HCl, pH 7.5, 100 mmol/L NaCl, 25 mmol/L $MgCl_2$, 1 mmol/L EDTA, and 0.1% protease-free bovine serum albumin) and homogenized in a glass tissue grinder. Total protein in the membrane preparation containing Smo was determined using the Pierce BCA protein assay (Pierce Chemical).

For the competitive binding assay, 100 μL of assay buffer was added to a 96-well GF/B filter plate (Millipore) for 10 minutes to pre-wet the filter and then removed. The following reagents were then added: 20 μL of assay buffer, 10 μL serial dilutions of compound, 20 μL of ^{3}H-Smo antagonist (3 nmol/L final concentration), and 50 μL of membrane preparation (40 μg total protein). The plates were incubated at room temperature for 2 hours, then washed and vacuum dried. The plates were then dried for 1 hour in a 60°C oven before the addition of 45 μL of Microscint 20 (Packard) and incubated at room temperature for 30 minutes to 1 hour, then counted in a TopCount scintillation counter (Perkin Elmer).

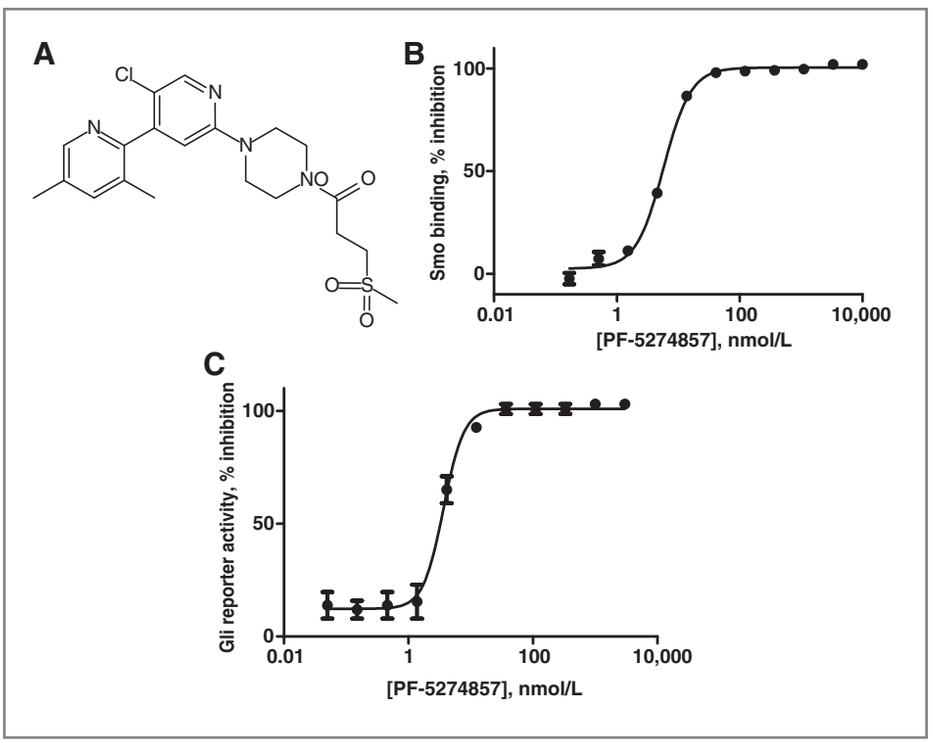

Figure 1. Inhibition of smoothened by PF-5274857. A, chemical structure of PF-5274857. B, concentration-dependent competitive binding of PF-5274857 to human Smo (amino acid 181–787). C, inhibition of Gli transcription in Gli-luciferase reporter assay in MEF cells. Each point represents the mean of duplicate measurements ± SE. The curves represent the best fit of data to 4-parameter sigmoidal dose–response equation (Prism, GraphPad).

The data were analyzed using GraphPad Prism software. Nonspecific binding was determined in the presence of ^{3}H-Smo antagonist (3 nmol/L), cold Smo-antagonist (30 μmol/L), and Smo membrane. The specific binding was obtained by subtraction of nonspecific binding from the total binding and used for the calculation of percentage inhibition in the presence of compound. The IC_{50} value was determined by fitting the percentage inhibition data to the 4-parameter fit equation for sigmoidal dose–response curve (variable slope). The K_i value was calculated using Cheng–Prusoff equation: $K_i = IC_{50}/[1+([L]/K_d)]$, where L is the concentration of ^{3}H-Smo antagonist (3 nmol/L), and K_d is the equilibrium dissociation constant of ^{3}H-Smo antagonist determined previously (12 nmol/L).

To evaluate the selectivity of the compound, PF-5274857 was profiled *in vitro* against a broad panel of receptors, enzymes, and ion channels at a concentration of 10 μmol/L (Cerep). In addition, it was profiled in an Invitrogen kinase selectivity panel (Invitrogen) including more than 150 kinases covering broad classes of protein kinases.

Gli-Luc reporter assay

Gli-Luc/MEF cells were grown in the knockout DMEM (Invitrogen) supplemented with 10% heat-inactive FBS (Hyclone), 2 mmol/L L-glutamine (Invitrogen), and 0.55 mmol/L β-mercaptoethanol until 90% confluence. On day 1, cells were trypsinized and seeded into white 384-well plates (Corning) in 20 μL per well of OptiMEM media (Invitrogen) that was supplemented with 1% heat-inactive FBS and 1 mmol/L sodium pyruvate at a concentration of 7,500 cells per well. Plates were incubated at 37°C and 5% CO_2 overnight. On day 2, PF-5274857 was added to the cells at a final concentration ranging from 3 μmol/L to 50 pmol/L at a 3-fold serial dilution followed by addition of recombinant mouse Sonic Hedgehog (Shh, R&D Systems) to a final concentration of 2 μg/mL. The cells were incubated with compounds and Shh for 48 hours at 37°C and 5% CO_2. Luciferase assays were conducted on day 4 using the Bright-Glo Luciferase Assay System (Promega) according to manufacturer's protocol. Briefly, Bright-Glo luciferase reagent (25 μL) was added to each well of the 384-well plate containing media. Plates were kept at room temperature for 5 minutes and then read on an Envision Luminescence plate reader (Perkin-Elmer). The IC_{50} value of PF-5274857 was calculated using GraphPad Prism.

Tumor growth inhibition and correlation of PK and PD studies in medulloblastoma allograft models

Severe combined immunodeficient (SCID)-beige mice (6–8 weeks old) were obtained from Charles River Laboratories. Animals were maintained under standard clean room conditions in accordance with the Pfizer Institutional Animal Care and Use Committee.

The medulloblastoma mouse model was genetically engineered to contain heterozygous deletion of Hh pathway repressor Ptch combined with either heterozygous or homozygous deletion of tumor suppressor p53 as previously described (27, 28). Medulloblastoma allograft mice were generated by subcutaneously implanting a small fragment of the primary $Ptch^{+/-}p53^{+/-}$ or $Ptch^{+/-}p53^{-/-}$ medulloblastoma tumor into the flank of SCID-beige mice. After a second passage, allograft mice bearing tumors ranging in size 350 to 700 mm^3 were randomized and enrolled into groups for tumor growth inhibition (TGI) and PK/PD studies. Tumor volume was measured by Preisser calipers and calculated using the formula: length × width^2 × 0.5.

To study the TGI, PF-5274857 (0, 1, 5, 10, and 30 mg/kg) was orally administered once a day to medulloblastoma allograft mice ($n = 6$). Animals were dosed for 6 consecutive days and tumor volume was measured daily. On the last day of dosing, animals were euthanized 6 hours postdose, and plasma and tumors were collected for drug exposure analysis and Hh pathway gene expression analysis (tumors). The percentage of TGI on day 6 was calculated on the basis of the following equation:

$$\%\ \mathrm{TGI} = \left[1-\left(V_{\mathrm{day6}}-V_{\mathrm{day0}}\right)/\left(V_{\mathrm{vehicle,day6}}-V_{\mathrm{vehicle,day0}}\right)\right]\times 100$$

where V_{day6} and V_{day0} refer to the tumor volume for the treated group on days 6 and 0, and $V_{vehicle,\ day6}$ and $V_{vehicle,day0}$ refer to the tumor volume for the vehicle group (0.5% methylcellulose) on days 6 and 0, respectively.

The correlation of PK and PD was studied in both $Ptch^{+/-}p53^{+/-}$ and $Ptch^{+/-}p53^{-/-}$ medulloblastoma allograft mice. Animals were dosed once with PF-5274857 at 0, 5, 10, and 30 mg/kg ($n = 3$). Both tumor samples and skin biopsies (6 mm^3) were taken at 2, 6, 12, and 20 hours postdose for exposure and Hh pathway genes expression analysis, and plasma samples were taken for exposure analysis.

Total RNA was extracted from the tumor tissue or skin biopsies using the RNeasy Mini Kit (Qiagen). Subsequently, cDNA was synthesized from the RNA using High Capacity cDNA Reverse Transcription Kit (Applied Biosystems) according to the vendor's protocol. Quantitative real-time PCR analysis of Hh pathway genes expression was conducted using ABI Prism 7900 sequence detection system (Applied Biosystems). The primers were obtained from Applied Biosystems.

PK/PD modeling

The PK, Gli1 mRNA biomarker, and TGI data were quantified using a naive-pooled PK/PD modeling approach. Models were fit to data using the SAAM II software (University of Washington, Seattle, WA). A one-compartment linear PK model adequately captured mouse PK profiles over the doses of 1 to 30 mg/kg of PF-5274857. The absorption phase was not captured by the data therefore an infusion model was used. To quantify the tumor and skin Gli1 mRNA response, an indirect response model was used with the drug effect being placed on the Gli1 mRNA production rate and

incorporated using a sigmoid E_{max} function. The skin Gli1 mRNA response displayed a larger variation, therefore data points greater than 200% of vehicle were excluded from the analysis, which resulted in the exclusion of 4 of 30 total data points. The tumor volume data were described by an exponential model with first-order growth and death rates. An empirical power function was developed to relate the biomarker response to the tumor volume data by incorporating the biomarker modulation on the tumor growth rate parameter. A percentage of TGI was used to summarize the tumor response at the end of the treatment regimen.

Brain uptake of PF-5274857

Approximately 10-week-old (250 g body weight) Wistar rats were dosed once with 10 mg/kg of PF-5274857 subcutaneously. Rats were euthanized 1 and 4 hours postdose ($n = 3$). Plasma, whole brain, and cerebrospinal fluid (CSF) were collected, and drug concentrations were analyzed using liquid chromatography/tandem mass spectrometry methods. The concentration of drug in whole brain was normalized by brain weight. To calculate the unbound plasma concentrations, the total plasma concentrations were multiplied by 0.067, a previously determined unbound fraction of rat plasma protein binding.

Modulation of Hh pathway genes in the brain of primary medulloblastoma mice by PF-5274857

Six-week-old $Ptch^{+/-}p53^{-/-}$ primary medulloblastoma mice ($n = 3$) were treated with vehicle or 30 mg/kg of PF-5274857 once daily for 1 or 4 days by oral gavage. At 6 hours after last dose, mice were euthanized and tumor-bearing cerebella were removed. Total RNA was extracted from the tumor tissue, and the expression levels of Hh pathway genes were analyzed quantitatively as described above.

Survival studies in primary medulloblastoma mice

Five-week-old $Ptch^{+/-}p53^{-/-}$ primary medulloblastoma mice were enrolled into 2 groups treated with either vehicle ($n = 15$) or 30 mg/kg of PF-5274857 ($n = 18$) once a day by oral gavage. The mice were monitored daily and euthanized if mice showed decreased mobility. The survival dates were recorded.

Bioluminescence imaging of brain Gli1 in Gli-luc transgenic mice treated with PF-5274857

Gli-luc transgenic mice were generated by microinjecting a construct containing 8 Gli binding sites fused to the δ-crystalin basal promoter and firefly luciferase gene as described previously (29). After the genotype of mice was confirmed, Gli-luc mice (5-week-old) were dosed orally once a day for 7 days with vehicle, 30 mg/kg, or 100 mg/kg PF-5274857 ($n = 4$–5). On day 7, at 6 hours postdose, mice were anesthetized and scalp was removed to expose the skull because skin with high expression of Gli may confound the brain measurement. Mice were also shaved for better exposure of Gli activity in the skin. Luminescence imaging was collected 25 minutes after intraperitoneal injection of luciferin (75 mg/kg) with 20 seconds exposure using an Ivis 200 Xenogen instrument. A region of interest encompassing the brain was defined manually and data were expressed as total photon Flux (photons/s).

Results

PF-5274857 is a potent and selective antagonist of Smo

The binding affinity of PF-5274857 to human Smo (amino acids 181–787) was determined in a ligand-displacement assay against a well-characterized ^{3}H-Smo antagonist (30). PF-5274857 was shown to bind to Smo with an IC_{50} of 5.8 ± 1.4 nmol/L (Fig. 1B). The K_i was calculated to be 4.6 ± 1.1 nmol/L.

PF-5274857 completely inhibits Shh-induced Hh pathway activity with an IC_{50} of 2.7 ± 1.4 nmol/L measured by the transcriptional activity of Smo downstream gene *Gli1* in MEF cells (Fig. 1C). This cellular potency against mouse Smo is nearly identical with an IC_{50} of 2.8 ± 1.5 nmol/L determined in NIH3T3 cells transiently transfected with human Smo. The comparable inhibition potency is consistent with the high homology in protein sequence between mouse and human Smo. Overall, the cellular activity of PF-5274857 correlates well with the binding potency of recombinant human Smo.

The selectivity profiling of PF-5274857 in the Cerep panel shows less than 50% inhibition of all receptors and enzymes at 10 μmol/L (Supplementary Table S1). Only the μ-opioid receptor was weakly inhibited by PF-5274857 with a dissociation constant of 36 μmol/L subsequently determined in a functional assay. Therefore, the selectivity window was more than 1,000-fold on the basis of the cellular IC_{50} value. Furthermore, PF-5274857 showed less than 20% inhibition against a broad panel of protein kinases at 1 μmol/L. Therefore, PF-5274857 was found to be a highly selective Smo antagonist.

PF-5274857 shows robust antitumor efficacy and correlation between PK and PD in medulloblastoma allograft mice models

The *in vivo* efficacy of PF-5274857 was evaluated in $Ptch^{+/-}p53^{+/-}$ medulloblastoma allograft mice. PF-5274857 showed significant dose-dependent TGI and induced tumor regression at high doses (≥10 mg/kg) after 6 days of treatment (Fig. 2A). On day 6, the calculated percentage of TGI was 39% ± 8% ($P = 0.4$), 80% ± 34% ($P = 0.1$), 119% ± 24% ($P = 0.003$), and 133% ± 32% ($P = 0.002$) at 1, 5, 10, and 30 mg/kg of PF-5274857, respectively. No body weight loss or other signs of illness were observed over the course of the study (Fig. 2B).

The effects of PF-5274857 on Hh pathway genes *Gli1*, *Gli2*, *Ptch1*, *Ptch2*, and *Smo* were measured in both tumor and skin in $Ptch^{+/-}p53^{-/-}$ medulloblastoma allograft mice in a single-dose study. As shown in Fig. 3A, in tumor tissue, PF-5274857 downregulated *Gli1*, *Gli2*, *Ptch1*, and

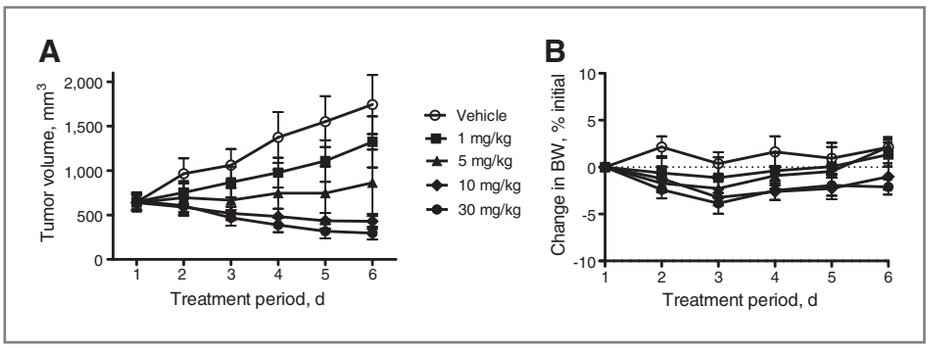

Figure 2. *In vivo* effects of PF-5274857 in Ptch$^{+/-}$p53$^{+/-}$ medulloblastoma allograft mice. Ptch$^{+/-}$p53$^{+/-}$ medulloblastoma allograft mice were dosed once daily for 6 days with PF-5274857 (0, 1, 5, 10, and 30 mg/kg). A, TGI. B, percentage change in body weight (BW). Each point represents the mean of measurements of 6 mice ± SE.

Ptch2 gene expression levels to various degrees with maximal effects being achieved between 6 and 12 hours postdose, whereas it had little effect on *Smo* levels. In skin tissue, downregulation of *Gli1* and *Gli2* was also observed with a similar time course (Fig. 3B), whereas changes in *Ptch1, Ptch2*, and *Smo* mRNA levels were minimal (data not shown). Among the Hh pathway genes evaluated here, *Gli1* displayed the most sensitive response to Smo inhibition and therefore was used as the PD marker for PK/PD correlation analysis.

The correlation of pharmacodynamic response of Gli1 mRNA expression with compound concentration in plasma was evaluated in both Ptch$^{+/-}$p53$^{+/-}$ and Ptch$^{+/-}$p53$^{-/-}$ medulloblastoma allograft mice. A mathematical model was developed that adequately described the PK/PD relationship and provided a quantification of the *in vivo* potency of PF-5274857 on the basis of Gli1 response. The model fit to the data for tumor Gli1 response in Ptch$^{+/-}$p53$^{+/-}$ and Ptch$^{+/-}$p53$^{-/-}$ medulloblastoma allograft mice are shown in Fig. 4A and B, respectively. The model-derived drug concentration for half maximal inhibition of the tumor Gli1 mRNA production rate (IC_{50}) by PF-5274857 was determined to be 8.9 ± 2.6 nmol/L in the Ptch$^{+/-}$p53$^{+/-}$ medulloblastoma allograft mice, which mathematically corresponds to tumor regression of 119% TGI after 6 days of plasma exposure at this concentration. In the Ptch$^{+/-}$p53$^{-/-}$ medulloblastoma allograft mice, the IC_{50} value was estimated to be 3.5 ± 0.5 nmol/L, consistent with the Ptch$^{+/-}$p53$^{+/-}$ results. The skin Gli1 mRNA response was more variable than that observed in the tumors largely because of the lower basal levels of Gli1 in skin of SCID-beige mice (Fig. 4C), which is reflected in the uncertainty around its estimated IC_{50} value (14 ± 8 nmol/L). This model fit to the TGI data is shown in Supplementary Fig. S1.

The mouse plasma exposure data are shown in Fig. 4D and were described by a monoexponential function with an apparent volume of distribution of 5.6 ± 0.5 L/kg and a half-life of 1.7 ± 0.1 hours. The compound exposures in the tumor and skin were also measured and showed the same time course as observed in the plasma (Supplementary Fig. S2). Overall, PF-5274857 displayed good oral bioavailability and low clearance in preclinical species.

PF-5274857 penetrates the blood–brain barrier

The concentrations of PF-5274857 in the CSF, brain, and plasma were measured, and the results are summarized in Table 1. Because PF-5274857 is not a P-glycoprotein substrate, it is sufficient to use the CSF concentrations as a surrogate to indicate unbound concentrations in the brain. To determine the extent of brain penetration, a ratio of the CSF concentration and the unbound plasma concentration was calculated. At 1 and 4 hours, the ratios were 0.43 ± 0.03 and 0.44 ± 0.1, respectively. The results indicate that approximately 40% of unbound PF-5274857 in the plasma was able to cross the blood–brain barrier in rats within 4 hours postdose.

In primary Ptch$^{+/-}$p53$^{-/-}$ medulloblastoma mice, the target modulation in the brain by PF-5274857 was characterized by measuring the expression levels of Hh pathway genes in the brain tumor at 6 hours postdose after 1 or 4 days of treatment. On day 1, no changes in gene

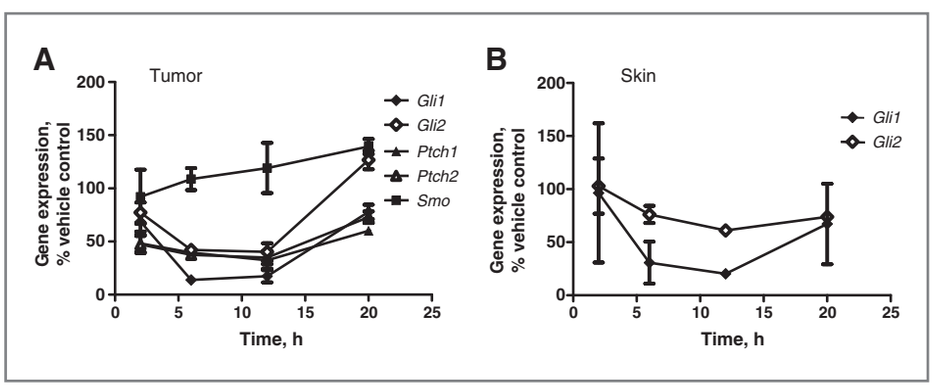

Figure 3. Modulation of Hh pathway genes in tumor (A) and skin (B) in Ptch$^{+/-}$p53$^{-/-}$ medulloblastoma allograft mice treated with a single dose of 30 mg/kg PF-5274857. The gene expression levels are expressed as percentage relative to the vehicle group. The results are mean values of measurements of 3 mice ± SE.

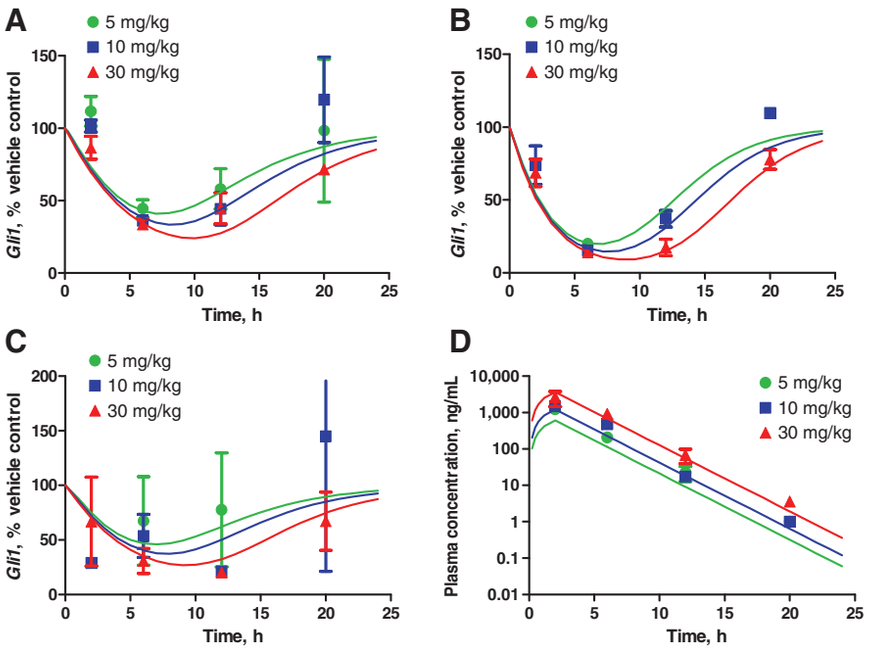

Figure 4. Pharmacokinetics and biomarker response in single dose study. All data were obtained following a single oral dose of PF-5274857 (0, 5, 10, and 30 mg/kg). A, tumor Gli1 mRNA responses in $Ptch^{+/-}p53^{+/-}$ medulloblastoma allograft mice. B, tumor Gli1 mRNA responses in $Ptch^{+/-}p53^{-/-}$ medulloblastoma allograft mice. C, skin Gli1 mRNA responses in $Ptch^{+/-}p53^{-/-}$ medulloblastoma allograft mice. D, total plasma concentrations. Each point represents the mean of measurements of 3 mice ± SE. The lines represent the model fit.

expression of *Gli1*, *Gli2*, *Smo*, *Ptch1*, and *Ptch2* were observed (data not shown). On day 4, *Gli1*, *Gli2*, *Smo*, and *Ptch2* expression levels were significantly downregulated at higher doses as shown in Fig. 5A. The *Ptch1* gene expression was marginally affected, consistent with the previous observation (31). The most significant change was observed in *Gli1* with a 20-fold reduction to 4.5% ± 0.4% of vehicle control. These results suggest that PF-5274857 was able to target Smo in the brain leading to the downregulation of Hh pathway activity in the brain tumor.

In the survival study, primary $Ptch^{+/-}p53^{-/-}$ medulloblastoma mice treated with 30 mg/kg of PF-5274857 had better survival rates than vehicle-treated mice (Fig. 5B; $P = 0.002$). All mice treated with vehicle developed lethargy because of brain tumors and were euthanized between 7 and 13 weeks. Four of 18 mice treated with PF-5274857 survived beyond 32 weeks and behaved normally.

Table 1. Exposures of PF-5274857 in the CSF, brain, and plasma in rats following a 10 mg/kg subcutaneous dose

	1 h	4 h
CSF, nmol/L	147 ± 27	165 ± 165
Brain, nmol/g	0.460 ± 0.119	0.513 ± 0.529
Plasma, nmol/L	5,130 ± 680	5,080 ± 4,070
Plasma, f_u, nmol/L	343 ± 46	341 ± 272
CSF/plasma, f_u[a]	0.43 ± 0.03	0.44 ± 0.10

NOTE: The results are the mean of measurements of 3 mice ± SD.
Abbreviation: f_u, fraction of unbound.
[a]Mean and SD were calculated from individual ratio values.

Because the brain tumor may disrupt the blood–brain barrier in primary medulloblastoma mice, nontumor-bearing Gli-luc transgenic mice were used to evaluate the penetration of PF-5274857 across the intact blood–brain barrier. Hh pathway activity in the brain can be readily monitored by optical imaging in Gli-luc transgenic mice. Images of treated and untreated mice are shown in Fig. 6A. The level of luciferase signal from the brain was quantified and showed significant reduction in mice treated with PF-5274857 in a dose-dependent manner (Fig. 6B), suggesting the suppression of Hh pathway activity in the brain of nontumor-bearing mice.

Discussion

Aberrantly activated Hh pathway signaling is thought to play a crucial role in the initiation and development of a number of cancers. Pharmacologic inhibition of Hh pathway activity by small-molecule inhibitors of Smo has generated encouraging therapeutic efficacy in the clinic, notably in basal cell carcinoma (32), and produced transient effects in medulloblastoma (33). Both tumor types are driven by Hh pathway mutations. Smo inhibitors are also being evaluated in other advanced tumors with overexpressed Hh ligand in clinical trials including hematologic malignancies, small cell lung, pancreatic, gastric cancers, and others (24). The clinical outcome for these tumor types remains to be seen.

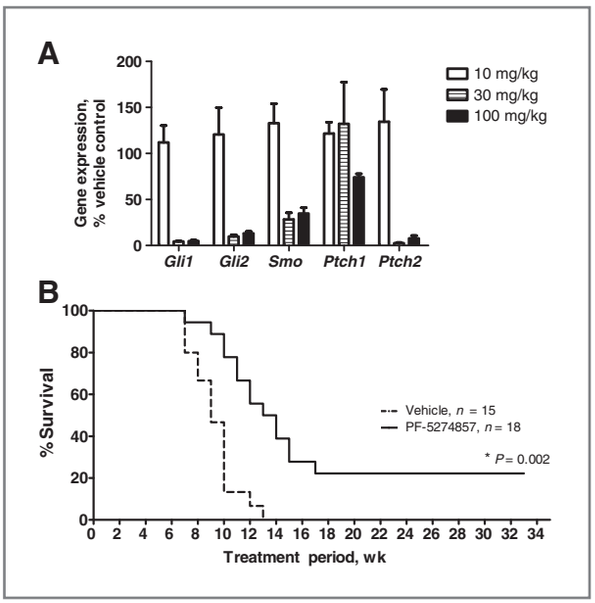

Figure 5. PF-5274857 penetrates blood–brain barrier in primary $Ptch^{+/-}p53^{-/-}$ medulloblastoma mice. A, effects of PF-5274857 on the expression levels of Hh pathway genes in brain tumor. Primary $Ptch^{+/-}p53^{-/-}$ medulloblastoma mice were treated with PF-5274857 (0, 10, 30, and 100 mg/kg) once daily by oral gavage for 4 days. The expression levels of genes in treated groups are shown as percentage relative to that in the vehicle group. The results are the average of measurements of 3 mice ± SE. B, treatment of primary $Ptch^{+/-}p53^{-/-}$ medulloblastoma mice with PF-5274857 increases the survival rates.

PF-5274857 is a novel Smo antagonist with high potency, selectivity, and robust antitumor activity in a $Ptch^{+/-}$ medulloblastoma tumor model driven by the activated Hh pathway. The expression levels of Hh pathway genes including *Gli1*, *Gli2*, *Ptch1*, and *Ptch2* in the tumor were effectively downregulated by PF-5274857 with *Gli1* being the most sensitive PD marker. Interestingly, the maximal response of PD markers was observed at 6 to 12 hours postdose, whereas the drug exposures in the plasma and the tumors peaked within 2 hours postdose. Similar delays in response were observed with other Smo antagonist with distinctly different chemical structures (data not shown). Therefore, the delay in maximal Hh pathway gene response is likely due to the time required for signal transduction following Smo binding, which reflects the underlying pharmacology of Smo signaling, and consequently was incorporated into the mathematical description of the data using an indirect response model (34). The mathematical characterization of the Gli1 mRNA PD response yielded consistent *in vivo* potencies in both $Ptch^{+/-}p53^{+/-}$ and $Ptch^{+/-}p53^{-/-}$ medulloblastoma allograft models ($IC_{50} = 8.9$ and 3.5 nmol/L, respectively), which are also in good agreement with the *in vitro* cellular IC_{50} (2.7 nmol/L). The consistent IC_{50} values suggest that *in vivo*, the drug can adequately access Smo and elicit a consistent pharmacologic effect.

To assess the *in vivo* potency of PF-5274857, we emphasize the use of tumor *Gli1*, a mechanistic marker over TGI, the outcome marker, as the primary PD parameter. This is due to the fact that tumor *Gli1* is a downstream gene of Smo signaling and its response is thought to more directly reflect the compound's mechanism of action on the Hh pathway. In contrast, the effects on tumor growth can be influenced by multiple factors such as tumor microenvironment and tumor types. Therefore, it is believed that Gli1 biomarker response will be more translatable to the clinic. In our studies, the downregulation of *Gli1* transcription was closely linked to the TGI in $Ptch^{+/-}$ medulloblastoma mice as captured in the mathematical model which uses the Gli1 mRNA response as the primary driver of the TGI response (see Supplementary Fig. S1 for the model fit to TGI data).

Despite tumor *Gli1* being an informative marker, the assessment of tumor *Gli1* sometimes can be hindered by the difficulty in obtaining tumor biopsies in a clinical setting. Because skin has an active Hh pathway and is

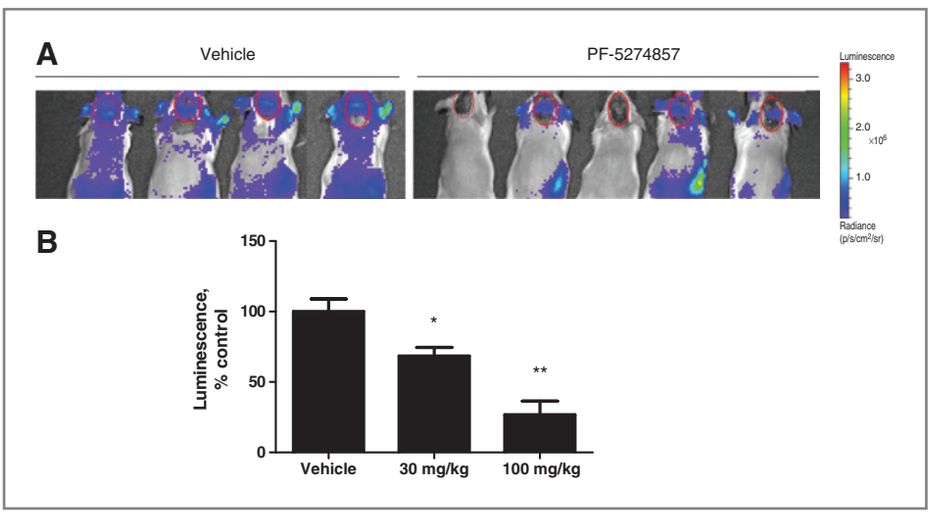

Figure 6. Imaging of Hh pathway in brain of Gli-luc transgenic mice. A, images of Gli-luc transgenic mice treated with either vehicle ($n = 4$) or PF-5274857 (100 mg/kg, $n = 5$) by oral gavage once a day for 7 days. Region of the brain circled by red line represented the area for luminescence quantification. B, quantification of Gli signal in the brain of Gli-luc transgenic mice treated with vehicle, 30 or 100 mg/kg PF-5274857. The results were the average ± SE. The Student *t* test was used to determine the *P* value (*, $P < 0.02$; **, $P < 0.002$).

easily accessible, we evaluated quantitatively the skin *Gli1* response to Smo inhibition by PF-5274857 in Ptch$^{+/-}$ medulloblastoma allograft SCID-beige mice. Here, we showed that the modulation of *Gli1* expressions and compound distribution follow the same pattern in both tumor and skin. The similarity in tumor and skin Gli1 IC_{50} values observed here in medulloblastoma tumor model supports the use of skin as a surrogate tissue for the measurement of the Gli1 biomarker.

One additional feature of PF-5274857 is its ability to cross the blood–brain barrier. PF-5274857 effectively inhibits Hh pathway activity in the brain and improves survival rates of primary medulloblastoma mice. The downregulation of *Gli1* in the brain tumor requires multiple dosing of PF-5274857, suggesting that the modulation of Hh pathway may require sufficient drug exposure levels accumulated over time in the brain. In primary medulloblastoma mice, 30 mg/kg of PF-5274857 achieved maximal downregulation of *Gli1* in the brain. In contrast, in nontumor-bearing mice, the same dose of PF-5274857 only generated moderate effects, and higher dose (100 mg/kg) was required to achieve similar level of *Gli1* modulation as that in medulloblastoma mice, implying a higher hurdle to cross the intact blood–brain barrier in nontumor-bearing mice. The penetration of blood–brain barrier makes PF-5274857 an attractive clinical candidate to treat brain tumors or metastasized brain tumors caused by an activated Hh pathway. For example, overexpression of Hh ligand is linked to small cell lung cancer which has high incidence of brain metastasis. Because the metastasized brain tumors maintain most of the characteristics of the primary tumor, PF-5274857 may provide effective clinical benefits in systemic treatment of such tumors.

In summary, PF-5274857 shows high potency and selectivity in the inhibition of Hh pathway activity *in vitro* and robust Gli1 mRNA modulation closely linked to antitumor efficacy *in vivo* with the additional feature of good brain penetration. PF-5274857 is orally available and metabolically stable *in vivo*. Taken together, the preclinical data suggest that PF-5274857 is a potentially attractive clinical candidate for treating tumor types driven by an activated Hh pathway including brain tumors and brain-metastasized tumors.

Disclosure of Potential Conflicts of Interest

All authors are current or former employees of Pfizer.

Acknowledgments

The authors thank Elena Dovalsantos, Jay Srirangam, Anand Sistla, Kim Kelso, and Todd VanArsdale for insightful discussion and support, and Steve Grant for critical reading of the manuscript.

The costs of publication of this article were defrayed in part by the payment of page charges. This article must therefore be hereby marked *advertisement* in accordance with 18 U.S.C. Section 1734 solely to indicate this fact.

Received September 2, 2011; revised October 24, 2011; accepted October 31, 2011; published OnlineFirst November 14, 2011.

References

1. Ingham PW, McMahon AP. Hedgehog signaling in animal development: paradigms and principles. Genes Dev 2001;15:3059–87.
2. Taipale J, Cooper MK, Maiti T, Beachy PA. Patched acts catalytically to suppress the activity of Smoothened. Nature 2002;418:892–7.
3. Kalderon D. Transducing the hedgehog signal. Cell 2000;103:371–4.
4. Teglund S, Toftgard R. Hedgehog beyond medulloblastoma and basal cell carcinoma. Biochim Biophys Acta 2010;1805:181–208.
5. Gailani MR, Stahle-Backdahl M, Leffell DJ, Glynn M, Zaphiropoulos PG, Pressman C, et al. The role of the human homologue of *Drosophila* patched in sporadic basal cell carcinomas. Nat Genet 1996;14:78–81.
6. Reifenberger J, Wolter M, Knobbe CB, Kohler B, Schonicke A, Scharwachter C, et al. Somatic mutations in the PTCH, SMOH, SUFUH and TP53 genes in sporadic basal cell carcinomas. Br J Dermatol 2005;152:43–51.
7. Xie J, Murone M, Luoh SM, Ryan A, Gu Q, Zhang C, et al. Activating Smoothened mutations in sporadic basal-cell carcinoma. Nature 1998;391:90–2.
8. Reifenberger J, Wolter M, Weber RG, Megahed M, Ruzicka T, Lichter P, et al. Missense mutations in SMOH in sporadic basal cell carcinomas of the skin and primitive neuroectodermal tumors of the central nervous system. Cancer Res 1998;58:1798–803.
9. Pietsch T, Waha A, Koch A, Kraus J, Albrecht S, Tonn J, et al. Medulloblastomas of the desmoplastic variant carry mutations of the human homologue of *Drosophila* patched. Cancer Res 1997;57:2085–8.
10. Raffel C, Jenkins RB, Frederick L, Hebrink D, Alderete B, Fults DW, et al. Sporadic medulloblastomas contain *PTCH* mutations. Cancer Res 1997;57:842–5.
11. Xie J, Johnson RL, Zhang X, Bare JW, Waldman FM, Cogen PH, et al. Mutations of the PATCHED gene in several types of sporadic extracutaneous tumors. Cancer Res 1997;57:2369–72.
12. Lauth M, Toftgard R. Hedgehog signaling and pancreatic tumor development. Adv Cancer Res 2011;110:1–17.
13. Tian H, Callahan CA, DuPree KJ, Darbonne WC, Ahn CP, Scales SJ, et al. Hedgehog signaling is restricted to the stromal compartment during pancreatic carcinogenesis. Proc Natl Acad Sci U S A 2009;106:4254–9.
14. Thayer SP, di Magliano MP, Heiser PW, Nielsen CM, Roberts DJ, Lauwers GY, et al. Hedgehog is an early and late mediator of pancreatic cancer tumorigenesis. Nature 2003;425:851–6.
15. Feldmann G, Dhara S, Fendrich V, Bedja D, Beaty R, Mullendore M, et al. Blockade of hedgehog signaling inhibits pancreatic cancer invasion and metastases: a new paradigm for combination therapy in solid cancers. Cancer Res 2007;67:2187–96.
16. Feldmann G, Habbe N, Dhara S, Bisht S, Alvarez H, Fendrich V, et al. Hedgehog inhibition prolongs survival in a genetically engineered mouse model of pancreatic cancer. Gut 2008;57:1420–30.
17. Zhao C, Chen A, Jamieson CH, Fereshteh M, Abrahamsson A, Blum J, et al. Hedgehog signalling is essential for maintenance of cancer stem cells in myeloid leukaemia. Nature 2009;458:776–9.
18. Dierks C, Beigi R, Guo GR, Zirlik K, Stegert MR, Manley P, et al. Expansion of Bcr-Abl-positive leukemic stem cells is dependent on Hedgehog pathway activation. Cancer Cell 2008;14:238–49.
19. Watkins DN, Berman DM, Burkholder SG, Wang B, Beachy PA, Baylin SB. Hedgehog signalling within airway epithelial progenitors and in small-cell lung cancer. Nature 2003;422:313–7.
20. Vestergaard J, Pedersen MW, Pedersen N, Ensinger C, Tumer Z, Tommerup N, et al. Hedgehog signaling in small-cell lung cancer: frequent *in vivo* but a rare event *in vitro*. Lung Cancer 2006;52:281–90.
21. Rubin LL, de Sauvage FJ. Targeting the Hedgehog pathway in cancer. Nat Rev Drug Discov 2006;5:1026–33.

22. Gupta S, Takebe N, Lorusso P. Targeting the Hedgehog pathway in cancer. Ther Adv Med Oncol 2010;2:237–50.
23. Robarge KD, Brunton SA, Castanedo GM, Cui Y, Dina MS, Goldsmith R, et al. GDC-0449-a potent inhibitor of the hedgehog pathway. Bioorg Med Chem Lett 2009;19:5576–81.
24. Mas C, Ruiz i Altaba A. Small molecule modulation of HH-GLI signaling: current leads, trials and tribulations. Biochem Pharmacol 2010;80: 712–23.
25. Low JA, de Sauvage FJ. Clinical experience with Hedgehog pathway inhibitors. J Clin Oncol 2010;28:5321–6.
26. Borzillo GV, Lippa B. The Hedgehog signaling pathway as a target for anticancer drug discovery. Curr Top Med Chem 2005;5: 147–57.
27. Wetmore C, Eberhart DE, Curran T. The normal patched allele is expressed in medulloblastomas from mice with heterozygous germ-line mutation of patched. Cancer Res 2000;60: 2239–46.
28. Wetmore C, Eberhart DE, Curran T. Loss of p53 but not ARF accelerates medulloblastoma in mice heterozygous for patched. Cancer Res 2001;61:513–6.
29. Kimura H, Ng JM, Curran T. Transient inhibition of the Hedgehog pathway in young mice causes permanent defects in bone structure. Cancer Cell 2008;13:249–60.
30. Frank-Kamenetsky M, Zhang XM, Bottega S, Guicherit O, Wichterle H, Dudek H, et al. Small-molecule modulators of Hedgehog signaling: identification and characterization of Smoothened agonists and antagonists. J Biol 2002;1:10.
31. Romer JT, Kimura H, Magdaleno S, Sasai K, Fuller C, Baines H, et al. Suppression of the Shh pathway using a small molecule inhibitor eliminates medulloblastoma in Ptc1(+/–)p53(–/–) mice. Cancer Cell 2004;6:229–40.
32. Von Hoff DD, LoRusso PM, Rudin CM, Reddy JC, Yauch RL, Tibes R, et al. Inhibition of the hedgehog pathway in advanced basal-cell carcinoma. N Engl J Med 2009;361:1164–72.
33. Rudin CM, Hann CL, Laterra J, Yauch RL, Callahan CA, Fu L, et al. Treatment of medulloblastoma with hedgehog pathway inhibitor GDC-0449. N Engl J Med 2009;361:1173–8.
34. Derendorf H, Meibohm B. Modeling of pharmacokinetic/pharmacodynamic (PK/PD) relationships: concepts and perspectives. Pharm Res 1999;16:176–85.